

NO-A167 017

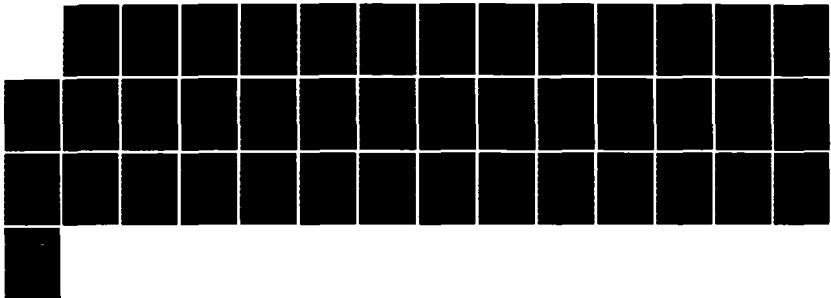
STRATIION EFFECT ON HF SIGNALS(U) SRI INTERNATIONAL
MENLO PARK CA G H PRICE 01 JUN 95 DWA-TR-05-250
DNA001-83-C-0413

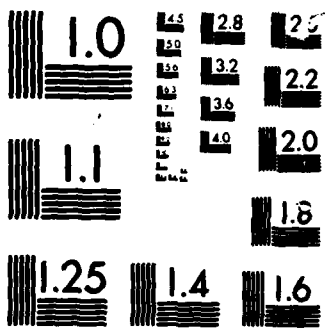
1/1

UNCLASSIFIED

F/G 20/14

ML





MICROCOPY

CHART

12

DNA-TR-85-250

STRIATION EFFECT ON HF SIGNALS

Gary H. Price
SRI International
333 Ravenswood Avenue
Menlo Park, CA 94025-3434

1 June 1985

Technical Report

CONTRACT No. DNA 001-83-C-0413

Approved for public release;
distribution is unlimited.

THIS WORK WAS SPONSORED BY THE DEFENSE NUCLEAR AGENCY
UNDER RDT&E RMSS CODE B322083466 S99QMXBB00027 H2590D.

Prepared for
Director
DEFENSE NUCLEAR AGENCY
Washington, DC 20305-1000

DTIC
ELECTE
APR 25 1986
*B

AD-A167 017

DTIC FILE COPY

86 4 25 006

UNCLASSIFIED

SECURITY CLASSIFICATION OF THIS PAGE

AD-A167017

REPORT DOCUMENTATION PAGE

1a REPORT SECURITY CLASSIFICATION UNCLASSIFIED		1b RESTRICTIVE MARKINGS	
2a SECURITY CLASSIFICATION AUTHORITY N/A since Unclassified		3 DISTRIBUTION AVAILABILITY OF REPORT Approved for public release; distribution is unlimited.	
2b DECLASSIFICATION DOWNGRADING SCHEDULE N/A since Unclassified			
4 PERFORMING ORGANIZATION REPORT NUMBER(S) SRI Project 6381		5 MONITORING ORGANIZATION REPORT NUMBER(S) DNA-TR-85-250	
6a NAME OF PERFORMING ORGANIZATION SRI International	6b OFFICE SYMBOL (If applicable)	7a NAME OF MONITORING ORGANIZATION Director Defense Nuclear Agency	
6c ADDRESS (City, State, and ZIP Code) 333 Ravenswood Avenue Menlo Park, CA 94025-3434		7b ADDRESS (City, State, and ZIP Code) Washington, DC 20305-1000	
8a NAME OF FUNDING SPONSORING ORGANIZATION	8b OFFICE SYMBOL (If applicable)	9 PROCUREMENT INSTRUMENT IDENTIFICATION NUMBER DNA 001-83-C-0413	
9c ADDRESS (City, State, and ZIP Code)		10 SOURCE OF FUNDING NUMBERS	
		PROGRAM ELEMENT NO 62715H	PROJECT NO S99QMXB
		TASK NO B	WORK UNIT ACCESSION NO DH007065
11 TITLE (Include Security Classification) STRIATION EFFECT ON HF SIGNALS			
12 PERSONAL AUTHOR(S) Price, Gary H.			
13a TYPE OF REPORT Technical	13b TIME COVERED FROM 830908 TO 840508	14 DATE OF REPORT (Year Month Day) 850601	15 PAGE COUNT 40
16 SUPPLEMENTARY NOTES This work was sponsored by the Defense Nuclear Agency under RDT&E RMSS Code B322083466 S99QMXBB00027 H2590D.			
17 COSAT CODES		18 SUBJECT TERMS (Continue on reverse if necessary and identify by block number)	
FIELD	GROUP	SUB-GROUP	
17	02	.1	High-frequency Radio-wave Propagation, Forward Scatter
20	14		Ionospheric Propagation, HF-channel Model
			HF Sky-wave Propagation, HF Propagation
19 ABSTRACT (Continue on reverse if necessary and identify by block number) Methods are described for calculating the effects of forward scatter by ionospheric irregularities on high-frequency sky-wave radio signals. The approach combines the forward-scatter theory (developed to treat refracted-ray paths in the context of acoustic propagation in oceans) with the model of ionospheric irregularities developed by the Defense Nuclear Agency. Expressions are given for calculating signal decorrelation in time, space, and frequency. <i>Price, Gary H.</i>			
20 DISTRIBUTION AVAILABILITY OF ABSTRACT <input type="checkbox"/> UNCLASSIFIED UNLIMITED <input checked="" type="checkbox"/> SAME AS RPT <input type="checkbox"/> DTIC USERS		21 ABSTRACT SECURITY CLASSIFICATION UNCLASSIFIED	
22a NAME OF RESPONSIBLE INDIVIDUAL Betty L. Fox		22b TELEPHONE (Include Area Code) (202) 325-7042	22c OFFICE SYMBOL DNA/STTI

DD FORM 1473, 84 MAR

83 APR edition may be used until exhausted
All other editions are obsolete

SECURITY CLASSIFICATION OF THIS PAGE

UNCLASSIFIED

UNCLASSIFIED

SECURITY CLASSIFICATION OF THIS PAGE

18. SUBJECT TERMS (Continued)

HF-scatter Model

Scatter-propagation Model

SUMMARY

Methods have been described for evaluating the major effects on HF sky-wave signals of forward scatter from ionospheric irregularities. The approach used to obtain these results combines the scatter theory that Flatté, et al.¹, developed for refracted ray paths and that developed under DNA sponsorship^{2,3} for transionospheric radio-wave propagation. The effects addressed by the theory include angular spread/spatial decorrelation, frequency (Doppler) spread/time decorrelation, and time spread/frequency decorrelation. The latter two of these effects, frequency spread and time spread, are those conventionally represented by the channel-scattering function. Angular spread is of concern to the HF system analyst for systems with narrow-beam antennas or spatial-diversity capabilities.

The results presented here incorporate a number of simplifications thought to be appropriate in applying the theory in a system context. Improving approximations in this spirit (e.g., to provide a better representation of the vertical profile of ionospheric electron-density) would in many cases be straightforward, but, at the expense of additional complexity in the algebraic detail.

A number of areas merit further attention. Evaluating the frequency coherence bandwidth (Section 7) may well require elaboration. However, evaluating the theory in its present form would seem appropriate first. The HF propagation experiment currently being undertaken by SRI International under DNA sponsorship addresses this need. Comparing the effects observed experimentally with those predicted by the present theory will provide the best guide to those areas in which further development will be worthwhile.

A question of recurring interest concerns propagation by means of paths reflected from nuclear plumes. These regions of enhanced,

structured ionization are produced by nuclear detonations in the upper atmosphere. The theory presented here appears capable (with a suitable redefinition of what is meant by "background ionosphere") of providing a means to assess some of the characteristics of such modes.

TABLE OF CONTENTS

<u>Section</u>	<u>Page</u>
SUMMARY	iii
LIST OF ILLUSTRATIONS	vi
LIST OF TABLES	vi
1 INTRODUCTION	1
2 IONOSPHERIC MODEL	4
3 UNPERTURBED RAY PATH	8
4 PHASE-STRUCTURE FUNCTION	11
5 SPATIAL DECORRELATION	17
6 TEMPORAL DECORRELATION	19
7 FREQUENCY DECORRELATION	21
8 EFFECTS IN A NOMINAL ENVIRONMENT	24
9 LIST OF REFERENCES	28



Accession For	
NTIS	✓
DTIC	
Unann.	
Justi	
By	
Distri	
Avail	
Dist	
A-1	

LIST OF ILLUSTRATIONS

<u>Figure</u>		<u>Page</u>
1	Conversion of rms Measures to Turbulent Strengths . .	6
2	Model Electron Density Profiles	25

LIST OF TABLES

<u>Table</u>		<u>Page</u>
1	Notation for Propagation Modeling	7
2	Parameter Values for a Sample Environment	24
3	Calculated Scatter Characteristics for a Sample Environment	26

SECTION 1

INTRODUCTION

Over the past decade,^{1*} it has been recognized that the scattering of signals by a randomly irregular medium can be characterized by integrals evaluated along the unscattered ray paths. This work can accommodate inhomogeneous random media, in which the ray path is refracted even in the absence of irregularities and anisotropic irregularity structures. The application of these results, together with the model of ionospheric irregularities developed by the Defense Nuclear Agency (DNA) for application to satellites,^{2,3} to the propagation of ionospherically refracted high-frequency (HF) radio waves is described in this final report for Contract DNA 001-83-C-0413.

In addition to developing procedures for calculating scatter effects reported here, this contract also included tasking to support the planning for the HF Channel Probe Experiment that was fielded successfully in Greenland by SRI International during the Fall of 1984. Developing the theory in conjunction with the experimental program has significantly enhanced the utility of both endeavors. Evaluating theory presented here through the comparison with the experimental results should be substantially easier because of the interaction between the experiment and the modeling development. Indeed, as a result of this interaction, selecting the quantities to be measured experimentally and specifying the particulars of their measurement were made with close attention to achieving meaningful and straightforward comparisons with theory.

*References are listed at the end of this report.

Three quantities generally suffice to characterize the effects of irregularities adequately for most system applications. These are the correlation between samples of the received signal separated (1) temporally, (2) spectrally (i.e., in frequency), and (3) spatially. Attention is first given to calculating the phase-structure function. This function is simply related to the spatial decorrelation of the signal phase on two paths separated by a small displacement at the receiver. This signal decorrelation between two separated receiving antennas determines the effectiveness of spatial diversity in improving system performance. The spatial correlation function is also directly related to the angular spread of the received signal. Although HF antennas are not easily made highly directive, some have been so designed, and the degree of angular spread relative to the antenna directivity remains an important parameter in assessing HF system performance.

The methods described for calculating the phase-structure function also pertain to calculating other scatter parameters. As will be shown, only minor modification of the procedure is necessary to obtain a description of the temporal decorrelation of the signal, given reasonable (with our present knowledge) simplifying assumptions. Indeed, the concept of the phase-structure function can be generalized to include separations in time and frequency as well as space.

Calculating the phase-structure function requires determining the path of the unscattered ray. Determining the sensitivity of the integrated phase along the path to a displacement of the path from its nominal (unscattered) position is also necessary. To facilitate these calculations, we have simplified the description of the background (i.e., unstructured) ionosphere somewhat. This simplification, described in Section 2, is a conventional one often employed in ionospheric radio-wave studies: The ionospheric electron-density distribution is assumed laterally uniform (i.e., the ionosphere is assumed stratified), and the form of the variation in electron density with height is chosen such that the refracted ray paths can be analytically described (Section 3). Thus, the computational burden imposed by incremental ray-trace solutions for the ray paths between

specified points have been avoided. We anticipated as well that our needs would have imposed precision requirements on an incremental ray-trace approach that substantially exceeded those normally encountered. With the analytic result, it is a simple matter, for small displacements, to determine the displacement to the ray path for any point along the path given a specified displacement of an end point, such as is needed for calculating the phase-structure function (Section 4), without repeating the entire path calculation.

Also described briefly in Section 2 is the model used to represent the irregularity structure of the ionosphere responsible for the effects of scatter. This model, which has been adapted from that developed as part of DNA's efforts to characterize the effects of scatter at higher frequencies, seems a reasonable starting point for describing the ionospheric structure important to HF. Elaboration or modification of the irregularity model may prove desirable as experience with the HF scatter model is gained. Because data are lacking with which to address this question at the present time, we will not address it here.

Characterizing the signal decorrelation in space, time, and frequency is discussed in Sections 5 through 7 after the development in Section 4 of methods for calculating the phase-structure function. We find that, as in the simpler case of transionospheric propagation at higher frequencies, a nominal value for the power-law index of the irregularity spectrum leads to a simple form for the spatial and temporal correlation functions. The decorrelation of the signal in space and time consequently can be simply characterized by decorrelation length (which, however, depends on direction) and decorrelation time, respectively. The relationship of the spatial decorrelation length to the angular extent of the signal, which is a more directly useful quantity in many cases, also is described.

SECTION 2
IONOSPHERIC MODEL

We have assumed that the unperturbed ionospheric electron density varies only with height. The form of this variation is considered quasi-parabolic, a choice that is analytically convenient without sacrificing practical utility. Specifically, we assume a spherically stratified profile of the form

$$N_e(r) = \begin{cases} \bar{N}_m [1 - \{(r-r_m)/y_m\}^2 (r_b/r)^2] & ; r_b \leq r \leq r_b r_m / (r_b - y_m) \\ 0 & ; \text{elsewhere} \end{cases} \quad (1)$$

in an earth-centered spherical polar-coordinate system with r the radial distance from the earth's center. The layer peak is located at r_m , with a peak density \bar{N}_m , and its base at r_b ; the layer's semithickness is $y_m = r_m - r_b$. For this profile, ray paths can be described analytically by a set of equations giving the angular distance along the earth's surface, $\theta(r)$, as a piecewise continuous function of r . As was noted in the introduction, the availability of these equations facilitates calculating the scatter parameters for the HF channel model.

The ionospheric irregularities are assumed anisotropic, as described by a three-dimensional power-law spatial spectrum of electron-density fluctuations of the form

$$\phi(q) = \frac{a' b' C_s}{(q_0^2 + q^2)^{\nu+1/2}}, \quad (2)$$

where q^2 is a quadratic form in the wave-number components K_x , K_y , and K_z ; ν is the power-law index; and a' and b' are elongation factors that describe the correlation lengths in the directions of the second and third principle axes relative to the shortest in the direction of the first. Here, a' describes the elongation parallel to the earth's magnetic field, and b' , that perpendicular to the geomagnetic meridian plane; both are normalized to the correlation length perpendicular to the field direction in the meridian plane.*

The parameter C_s is a measure of irregularity strength, and q_0 specifies the outer scale. The electron-density variance, σ_N^2 , can be obtained by integration of $\phi(q)$ over all q . The rms electron-density variation, σ_N , is considered a fixed fraction of the mean electron density, $\langle N_e \rangle$; such a relationship, although not essential to the model, is a reasonable approximation for the propagation environments of interest. With q_0 and N specified, C_s can be calculated from the formula

$$C_s = \frac{8\pi^{3/2} \sigma_N^2 q_0^{2\nu-2} \Gamma(\nu + 1/2)}{\Gamma(\nu - 1)}. \quad (3)$$

* The coefficients of K_x , K_y , and K_z depend on the coordinate system, as will be described shortly.

Figure 1 relates the numerical magnitudes of σ_N and C_s for various values of the outer scale $L = 1/q_0$.

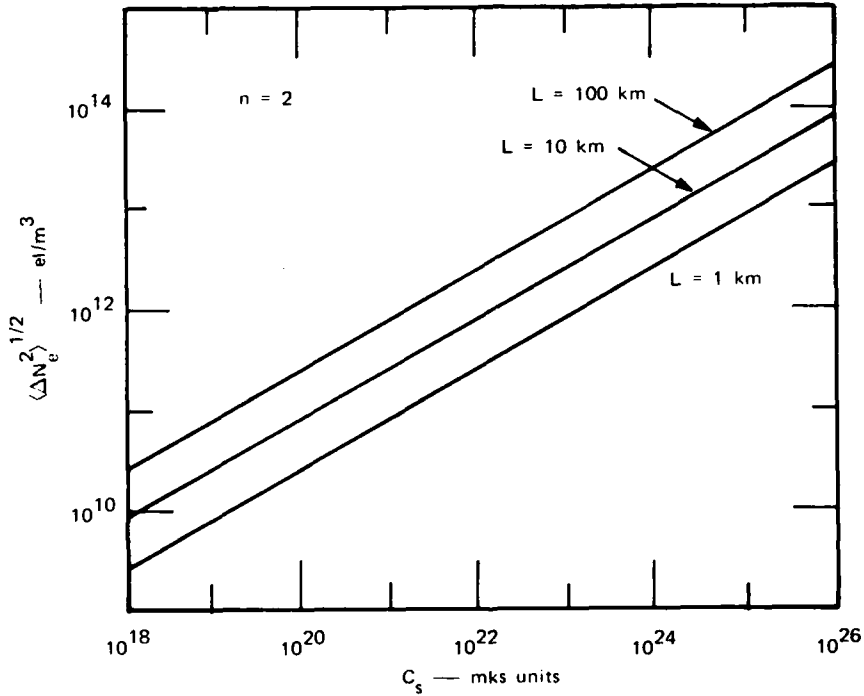


Figure 1. Conversion of rms measures to turbulent strengths.

The relationship of the parameters defined here to those employed by Wittwer² to model structured ionization is summarized in Table 1. The two models are formally identical.

Table 1. Notation for propagation modeling.

Natural Ionosphere	Wittwer ²	Comment
q_o	L_s^{-1}	Outer-scale wave number
a'	L_t/L_s	Axial ratio along field
b'	L_r/L_s	Transverse axial ratio
δ	θ	Orientation of transverse irregularity axis
G	$q_o L_z$	Geometric enhancement factor
ψ_{BP}^*	ϕ	Briggs-Parkin angle
$a q_o / G$	$L_u = L_s^2 (a^2 \cos^2 \phi + \sin^2 \phi)$	Briggs-Parkin factor
θ		Zenith angle
φ		Magnetic azimuth angle
$z_R \sec \theta$	$z_f = \frac{(z_T - z_1) z_1}{z_T}$	"Reduced" propagation distance
ν	$n = \nu + 1/2$	Spectral index parameter
$\phi_{\Delta N_e} \sim q^{-(2\nu+1)}$	$\phi_{\Delta N_e} \sim q^{2n}$	Form of three-dimensional spectral density function

* The Briggs-Parkin angle--the angle between the line of sight and the magnetic field--is given in terms of ψ , θ , and φ as

$$\cos \psi_{BP} = \cos \psi \sin \theta \cos \phi + \sin \psi \cos \theta$$

SECTION 3

UNPERTURBED RAY PATH

In order to compute the effects of structure, a description of the unperturbed ray path is needed. As will be described shortly, these computations involve, among other things, determining the extent to which the path is shifted by a displacement of its end points. Calculating this displacement is made easier by the form selected for the unperturbed electron-density profile, Eq. (1); this form allows the unperturbed path to be specified as an explicit function relating the signal frequency, profile parameters, and path coordinates. In this development, we have attempted to retain the notation of Croft and Hoogasian⁴ for the profile and path parameters.

Snell's law for a spherically stratified medium (also known as Bourger's rule) specifies generally that the local elevation angle of the ray, β , satisfies

$$\beta(r, \beta_0) = \arccos \left[r_0 \cos \beta_0 / (r \bar{\mu}(r)) \right] , \quad (4)$$

where β_0 is the ray elevation angle at the transmitter. The (unperturbed) mean refractive index, $\bar{\mu}$, is given by

$$\bar{\mu}^2(r) = 1 - \frac{e^2 N_e^2(r)}{\epsilon_0 \omega^2 m_e} . \quad (5)$$

For the region between the transmitter at $r_t = (r_0, 0, 0)$ and the base of the ionosphere at r_b , this relationship yields

$$\theta(r, \beta_0) = \beta(r, \beta_0) - \beta_0 , \quad r_0 \leq r \leq r_b ; \quad (6)$$

while within the ionosphere,

$$\begin{aligned} \theta(r, \beta_o) = & \beta_b(\beta_o) - \beta_o - \frac{r_o \cos \beta_o}{c^{1/2}(\beta_o)} \left\{ \ln[\mu(r) \sin \beta(r, \beta_o)] \right. \\ & + c^{1/2}(\beta_o)/r + b/(2c^{1/2}(\beta_o))] \\ & \left. - \ln[\sin \beta_b(\beta_o) + c^{1/2}(\beta_o)/r_b + b/(2c^{1/2}(\beta_o))] \right\}, \quad r_b \leq r \leq r_t \quad (7) \end{aligned}$$

with

$$\beta_b(\beta_o) = \beta(r_b, \beta_o) \quad (8)$$

and

$$c(\beta_o) = (r_b r_m / (F y_m))^2 - r_o^2 \cos^2 \beta_o, \quad (9)$$

where

$$F = \frac{\omega}{\omega_c} \quad (10)$$

is the ratio of the wave angular frequency, ω , to the critical frequency

$$\omega_c^2 = \left(\frac{e^2 N_m}{\epsilon_o m e} \right). \quad (11)$$

The parameter b , not to be confused with the irregularity anisotropy parameter b' , is given by

$$b = -\frac{2}{r_m} (r_b r_m / (Fy_m))^2 \quad (12)$$

On the descending leg of the ray path, the corresponding expressions for θ are

$$\begin{aligned} \theta(r, \beta_o) = & \beta_b(\beta_o) - \beta_o - \frac{r_o \cos \beta_o}{c^{1/2}(\beta_o)} \left\{ \ln \left[\frac{b^2}{4c(\beta_o)} - a \right] \right. \\ & - \ln \left[\sin \beta_b(\beta_o) + \frac{c^{1/2}(\beta_o)}{r_b} + \frac{b}{2c^{1/2}(\beta_o)} \right] \\ & \left. - \ln \left[\mu(r) \sin \beta(r, \beta_o) + \frac{c^{1/2}(\beta_o)}{r} + \frac{b}{2c^{1/2}(\beta_o)} \right] \right\}, \quad r_b \leq r \leq r_t \quad (13) \end{aligned}$$

and

$$\begin{aligned} \theta(r, \beta_o) = & 2\beta_b(\beta_o) - \beta_o - \beta(r, \beta_o) - \frac{r_o \cos \beta_o}{c^{1/2}(\beta_o)} \left\{ \ln \left[\frac{b^2}{4c(\beta_o)} - a \right] \right. \\ & \left. - 2 \ln \left[\sin \beta_b(\beta_o) + \frac{c^{1/2}(\beta_o)}{r_b} + \frac{b}{2c^{1/2}(\beta_o)} \right] \right\}, \quad r_o \leq r \leq r_b \quad (14) \end{aligned}$$

where

$$a = 1 - \frac{1}{F^2} + (r_b / (Fy_m))^2 \quad (15)$$

again is not to be confused with the irregularity anisotropy factor a' . The height, r_t , of the ray apex is given by

$$a r_t^2 + b r_t + c = 0 \quad (16)$$

SECTION 4

PHASE-STRUCTURE FUNCTION

The mutual coherence function of a randomly scattered wavefield describes the wavefield decorrelation caused by the scatter. Spatial, temporal, and spectral decorrelation of the signal can all be important to a communication system and, therefore, need to be described in the channel model. Spatial decorrelation is conveniently expressed in terms of the phase-structure function, $D(\rho, \rho')$, which is defined as the mean square difference in the signal phase perturbation, $\delta\phi$, observed at two points, ρ and ρ' :

$$D(\Delta) = \langle [\delta\phi(\rho) - \delta\phi(\rho')]^2 \rangle, \quad (17)$$

where $\Delta = |\rho - \rho'|$ is the spatial separation between the points. Temporal coherence of the wavefield is also usefully discussed in terms of a similar quantity if the temporal variation of the propagation medium is simply equivalent to a uniform drift of the irregularities. We, therefore, first consider the evaluation of the phase-structure function. In following sections, we address using it and related quantities to characterize the signal decorrelation.

The phase-structure function can be approximately evaluated^{2, 5} as a sum over contributions from points along the unscattered ray path

$$D(\Delta^R) \cong \int_{\text{path}} ds d[\mathbf{r}; \Delta(\mathbf{r})] \quad (18)$$

where $\Delta^R = \Delta(\mathbf{r}_R) = \rho - \rho'$ is some spatial displacement at the receiver, located at \mathbf{r}_R , and $\Delta(\mathbf{r})$ is the corresponding displacement at some point, $\mathbf{r} = \mathbf{r}(s)$, on the ray path. The relationship of $\Delta(\mathbf{r})$ to Δ^R is discussed further below.

Because θ is given explicitly as a function of r by the ray-path equations, it is straightforward to express the phase-structure function, D , as an integral over r . The increment of path length is given by

$$ds = \frac{dr}{\sin \beta(r)}, \quad (19)$$

and $D(\Delta^R)$ can be written

$$D(\Delta^R) = \int_{r_b}^{r_t} dr \frac{d[r; \Delta(r)]}{\sin \beta(r)} + \int_{r_t}^{r_b} dr \frac{d[r; \Delta(r)]}{\sin \beta(r)}, \quad (20)$$

if we assume that the path segments between the earth's surface and the base of the ionosphere are free of irregularities.

The incremental contribution to the phase-structure function from each differential segment of the path can be viewed as equivalent to that from a phase screen representing the effects of the irregularities located within a layer of thickness $dL = dr/\tan\beta$. The general form of the phase-structure function for such a layer has been calculated by Rino⁶; formally, we equate this result to $d[r; \Delta(r)]ds$ to obtain

$$d[r; \Delta(r)] = \frac{r_e^2 \lambda^2 G(r) C_s(r) \Gamma(\nu - 1/2)}{2\pi \Gamma(\nu + 1/2)} \cdot \frac{1 - 2 \left(\frac{q_o y}{2}\right)^{\nu-1/2} \frac{K_{\nu-1/2}(q_o y)}{\Gamma(\nu - 1/2)}}{q_o^{2\nu - 1}} \quad (21)$$

where λ is the signal wavelength and r_e is the classical electron radius. $K_{\nu-1/2}$ is the modified Bessel function of imaginary arguments,

$$G = \frac{a^2 b^2}{(AC - B^2/4)^{1/2} \cos \beta} \quad (22)$$

and

$$y^2 = \frac{CA\Delta_\phi^2 - B\Delta_\phi\Delta_r + A\Delta_r^2}{AC - B^2/4} \quad (23)$$

with

$$A = \hat{C}_{11} \quad (24a)$$

$$B = 2 (\hat{C}_{12} - \tan|\beta|\hat{C}_{13}) \quad (24b)$$

$$C = \hat{C}_{22} - 2\hat{C}_{23} \tan|\beta| + \hat{C}_{33} \tan^2\beta \quad (24c)$$

providing the dependence of the scatter effects on the path orientation relative to the geomagnetic field. This dependence is introduced by the anisotropy of the irregularities.

Equation (21) can be approximated well by³

$$d[r; \Delta(r)] = G(r)C_{\delta\phi}^2 |y|^{\min(2\nu-1, 2)} \quad (25)$$

where

$$C_{\delta\phi}^2 = \frac{\lambda^2 r_e^2 C_s}{2\pi} \left(\nu^2 - \frac{9}{2}\nu + \frac{11}{2} \right) \quad (26)$$

An equivalent approximation has been derived by Wittwer.^{2,7}

The \hat{C}_{ij} are the elements of a transformation matrix for normalization of a quadratic form that appears in the anisotropy model.³ For our geometry,

$$\hat{C}_{11} = (\sin^2 \psi + a^{-2} \cos^2 \psi) \sin^2 \delta + b^{-2} \cos^2 \delta \quad (27a)$$

$$\hat{C}_{22} = \cos^2 \psi + a^{-2} \sin^2 \psi \quad (27b)$$

$$\hat{C}_{33} = (\sin^2 \psi + a^{-2} \cos^2 \psi) \cos^2 \delta + b^{-2} \sin^2 \delta \quad (27c)$$

$$\hat{C}_{12} = (1 - a^{-2}) \sin \psi \cos \psi \sin \delta \quad (27d)$$

$$\hat{C}_{13} = (\sin^2 \psi + a^{-2} \cos^2 \psi - b^{-2}) \sin \delta \cos \delta \quad (27e)$$

$$\hat{C}_{23} = (1 - a^{-2}) \sin \psi \cos \psi \cos \delta \quad , \quad (27f)$$

where ψ is the dip angle of the geomagnetic field, and δ is the angle between the geomagnetic meridian plane and that containing the path. A positive δ is taken to rotate θ into ϕ as the path plane is rotated about \hat{i}_r into the geomagnetic meridian plane.

Given a displacement $\Delta^R = (\Delta_\phi^R, \Delta_r^R, \Delta_\theta^R)$ at the receiver, the Δ_r and Δ_ϕ are functions of the location on the ray path. First, the displacement Δ^R is reduced to that in the (r, ϕ) plane, $\Delta^\perp = (\Delta_\phi^\perp, \Delta_r^\perp)$ through the relationship

$$\Delta^\perp = (\Delta_\phi^R, \Delta_r^R + \tan \beta_o \Delta_\theta^R) \quad . \quad (28)$$

The displacement $\Delta_\phi(r)$ in the horizontal transverse coordinate is simply proportional to θ :

$$\Delta_\phi(r) = \frac{\theta(r)}{\theta_o} \Delta_\phi^\perp = \frac{\theta(r)}{\theta_o} \Delta_\phi^R \quad . \quad (29)$$

The displacement $\Delta r(r)$ in the vertical coordinate is less direct. Given $\theta(r, \beta_o)$, we have

$$d\theta = \frac{\partial \theta}{\partial r} dr + \frac{\partial \theta}{\partial \beta_o} d\beta_o \quad (30)$$

for the displacement in θ , given incremental changes in r and the take-off angle β_0 . For a fixed θ , $d\theta = 0$, and r is related to β_0 by

$$\frac{dr}{d\beta_0} = - \frac{(\partial\theta/\partial\beta_0)_r}{(\partial\theta/\partial r)_{\beta_0}} \quad (31)$$

For small Δ_r^\perp , then, the change in β_0 induced by the displacement Δ_r^\perp at θ_R causes a displacement $\Delta_r(r)$ at $\theta(r)$ given by

$$\Delta_r(r) = \frac{(dr/d\beta_0)|_{\theta(r)}}{(dr/d\beta_0)|_{\theta_R}} \Delta_r^\perp \quad (32)$$

or

$$\Delta_r(r) = + \frac{\frac{(\partial\theta/\partial\beta_0)_r}{(\partial\theta/\partial r)_{\beta_0}} \Big|_{\theta(r)}}{\frac{(\partial\theta/\partial\beta_0)_r}{(\partial\theta/\partial r)_{\beta_0}} \Big|_{\theta_R}} (\Delta_r^R + \tan \beta_0 \Delta_\theta^R) \quad (33)$$

Calculation of the partial derivatives of θ from the expressions given above for $\theta(r, \beta_0)$ is messy, but straightforward.

Only the practical difficulties involved in evaluation of the integrals for $D(\Delta^R)$ remain to be considered. At the path apex, $\beta = 0$. Consequently, we have to deal with an integrable singularity resulting from the $\sin \beta$ in the denominator. This is a purely geometric factor resulting from the projection of the path increment, ds , onto the vertical-axis integration increment, dr . The offending factor can be cast in the form

$$\frac{1}{\sin\beta(r)} = \frac{\mu(r)r}{(ar^2 + br + c)^{1/2}} \quad (34)$$

showing that, given the absence of any other singularities at r_t introduced by the remainder of the integrand, the singularity can be

integrated (cf., the integral forms for other path characteristics addressed by Croft and Hoogasian⁴). Although algebraically messy, expansion of the remainder of the integrand in a power series about r_t provides a straightforward approach to dealing with the singularity. This expansion is employed over only a limited portion of the integration range, with straightforward numerical integration employed over the remainder, to gain efficiency.

SECTION 5

SPATIAL DECORRELATION

Spatial decorrelation of the received signal is described directly by the phase structure function, $D(\Delta)$, defined in Eq. (17). Namely, the spatial autocorrelation function for the complex signal envelope is given by

$$R(\Delta) = e^{-\frac{1}{2}D(\Delta)} . \quad (35)$$

Although the spatial correlation function is of immediate interest in the assessment of spatial-diversity systems, the angular power spectrum of the received signal is usually more directly useful. The two quantities constitute a Fourier-transform pair when the angular spectrum is expressed in wave-number (k) space. Thus, one can readily be derived from the other, and both contain the same information.

For sufficiently small spatial displacements, the relationship between the displacement of the path end point and that of other points along the path is linear, as given by Eqs. (29) and (33). Equation (29) remains linear regardless. In the linear case, the dependence of $D(\Delta)$ on Δ is the same as that given by Eq. (25) for $d[r; \Delta(r)]$, the incremental contributions to D from different portions of the path. Thus, given the commonly assumed value of 1.5 for ν , the power-law index of the ionospheric irregularities, D is a quadratic function of Δ , and the autocorrelation function is, from Eq. (35), Gaussian in form.

The Fourier transforms relating angular power spectrum and spatial correlation function can readily be evaluated under these circumstances, yielding a Gaussian form (as a function of wave number, k) for the angular power spectrum as well. If we now characterize the spatial

decorrelation function in a particular direction by the value of Δ , denoted Δ_e , for which it has decreased to $1/e$ [i.e., $D(\Delta_e) = 2$], the half width of the angular spectrum in this direction, θ_e , again characterized by the $1/e$ point, is given by

$$\theta_e = \arcsin \frac{c}{\pi f \sqrt{\Delta_e}}, \quad (36)$$

where c is the speed of light and f is the frequency. The apparent complexity of Eq. (36) is a consequence of the width being expressed in terms of the angular variable, θ , rather than a component of the wave number, k .

SECTION 6

TEMPORAL DECORRELATION

Temporal decorrelation of the signal is caused by the evolution of the irregularities through which the signal propagates. It can be evaluated in a manner similar to that used to determine the spatial decorrelation, discussed in the previous section. For temporal decorrelation, however, the differences between the media encountered along the same path at two times, rather than those found between two paths at the same time, are of interest.

If a fixed spatial-irregularity structure is, as we assume, essentially convected across the path during the time necessary for the signal to decorrelate, the effect is the same as if the path were being shifted spatially. In this case, the calculation of the temporal decorrelation becomes very similar to that described previously for spatial decorrelation. To apply the calculation to temporal decorrelation, it is necessary only to modify the details about how the path is to be displaced in a suitable manner.

The simplest case is that of a uniform convection velocity at all points along the path. In this case, a uniform displacement of the entire path in the direction of the velocity vector, with the magnitude of the displacement proportional to time, is appropriate. The modification of the phase-structure-function calculation required to produce such a displacement is readily achieved by redefining the displacement parameter, y , of Eq. (23). This parameter is considered proportional to a time separation, Δt :

$$y = v_{\text{eff}} \Delta t \quad . \quad (37)$$

The proportionality constant v_{eff} constitutes an effective speed for drift of the irregularities across the path. For a drift in an arbitrary direction, $\mathbf{v} = (v_{\theta}, v_{\phi}, v_r)$, v_{eff} is given by

$$v_{\text{eff}}^2 = \frac{Cv_s^2 - Bv_s v_{\phi} v_r + Av_{s_r}^2}{AC - B^2/4}, \quad (38)$$

which corresponds roughly to Eq. (23). In Eq. (38),

$$\mathbf{v}_s = \mathbf{v}_{\perp} - \tan \beta \hat{\mathbf{a}}_{k_T} v_{\theta} \quad (39)$$

with $\mathbf{v}_{\perp} = (v_{\phi}, v_r)$, much as in Eq. (28). The vector $\hat{\mathbf{a}}_{k_T}$ in Eq. (39) is a unit vector in the r - ϕ plane that is directed along the projection of the wave-normal vector, \mathbf{k} , into this plane, β being the angle between \mathbf{k} and the perpendicular, directed along $\hat{\mathbf{i}}_{\phi}$, to this plane. Thus, $\hat{\mathbf{a}}_{k_T} = \pm \hat{\mathbf{i}}_r$, depending upon whether the portion of the ray going up (+) or going down (-) is being considered.

The temporal variation of the medium can also be discussed in terms of the distortion of the signal frequency spectrum (i.e., Doppler spread) that it produces. As in the case of the spatial-correlation function and angular power spectrum discussed in Section 5, the Fourier-transform relationship that connects the signal power spectrum and the time correlation function yields particularly simple results when the power-law index, ν , of the ionospheric irregularities [Eq. (2)] has a value of 1.5. Again, the form of both functions becomes Gaussian in this circumstance, and the $1/e$ decorrelation time, τ , and the spectral $1/e$ half width, f_D , are related in essentially the same manner as are their spatial counterparts:

$$f_D = \frac{1}{\pi\tau} \quad (40)$$

SECTION 7

FREQUENCY DECORRELATION

Decorrelation of the signal frequency spectrum and a corresponding time (delay) spread of the signal waveform also result from scatter by ionospheric irregularities. Several effects can be identified that may contribute to the delay spread. Two of these are familiar from the theory previously developed for unrefracted line-of-sight paths. The third, which bears a close relationship to the frequency spread and angular spread that have already been discussed in previous sections of this report, is potentially important only for refracted ray paths. Consequently, it appears not to have been considered previously.

We first note that time spread can result from the difference in travel time, or group delay, between the unscattered ray path and those that join the transmitter and receiver to scattering points lying to one side of the unscattered path. The magnitude of this component of the time spread is determined largely by the difference in geometric path length between the two paths.

Considerable simplification in calculating this delay-spread component can be achieved by observing that the constraints imposed by refraction on vertical displacement of the ray path severely limit the sensitivity of the signal to scatter by the vertical component of any irregularities present.¹ This insensitivity is further enhanced by irregularity structures, such as those encountered in the ionosphere at mid and high latitudes, that have much larger scales vertically than horizontally. Thus, to good approximation, we need consider only the lateral spread in the signal angular spectrum to determine this component of the delay spread. If we again assume that the significant scatterers are concentrated near midpath, a simple geometric estimate, ignoring earth curvature, of the delay spread, t_s , yields

$$\tau_s \cong \frac{D}{2c} \tan^2 \theta_e, \quad (41)$$

where D is the path length, and θ_e is the e^{-1} point on the lateral spread owing to scatter of the signal angular spectrum, which was discussed in Section 5.

We have assumed (for the present) that the major contribution to the delay spread will generally result from the effect just discussed. This expectation, however, remains to be placed on a firm footing. Thus, it seems appropriate to discuss briefly the other possible sources of delay spread and how they might be assessed.

Delay spread can also result from random fluctuations of the integrated electron density along the unscattered ray path. Such fluctuations on line-of-sight paths cause a corresponding fluctuation in the group delay that constitutes a delay spread. For refracted ray paths, however, the effect of such fluctuations separate less clearly from those associated with scatter from points to one side of the path, discussed above. It remains to be determined if a simple integration of the mean-square refractive-index fluctuations along the unscattered ray path will adequately describe this contribution to the delay spread.

A third component of the delay spread is most easily addressed in the frequency domain, as a frequency decorrelation. In contrast to the situation at higher frequencies, in which refraction is generally considered to be negligible, a shift in signal frequency at HF displaces the path to first order. This spatial separation implies a frequency decorrelation in consequence of the random spatial fluctuations of the medium through which the signal propagates.

This decorrelation can be evaluated in much the same way as is that from a spatial displacement of the receiver, namely, by calculating the phase-structure function, as discussed in Sections 4 and 5. The spatial separation produced at each point along the unperturbed ray path by a small frequency displacement is first determined. The incremental contribution to the phase-structure function from this displacement is

then integrated along the path. In this case, Eq. (17) now yields a frequency correlation function, the Fourier transform of which constitutes the third delay-spread component.

SECTION 8

EFFECTS IN A NOMINAL ENVIRONMENT

Sample calculations made in the course of implementing the model for use in conjunction with the HF Channel Probe experiment serve to illustrate the model. The results of some of these calculations are presented here. The values assumed for the model parameters in these calculations are given in Table 2. These values are representative of

Table 2. Parameter values for a sample environment.

Parameter	Value
ν	1.5
q_0	10^{-4} m^{-1}
a'	10
b'	1
$\langle \Delta N_e^2 \rangle / \bar{N}_e^2$	0.8
ν_{eff}	400 m/s

either the natural environment or one disturbed by a high-altitude nuclear detonation. The value of 0.8 assumed for the fluctuation variance is, however, probably excessively large for the natural environment. Measurements using the DNA HILAT satellite have, for example, shown 0.2 to be a more representative value for this parameter

in the polar-cap ionosphere,* which is a relatively severe example of naturally produced structure. The 400 m/s drift speed, on the other hand, is low for the nuclear environment; 1000 m/s might be more appropriate as a nominal value for the latter.

A number of calculations were made for a propagation path 1918 km in length (the length of the path instrumented experimentally) using the two profile models shown in Figure 2. Both models have vertical-

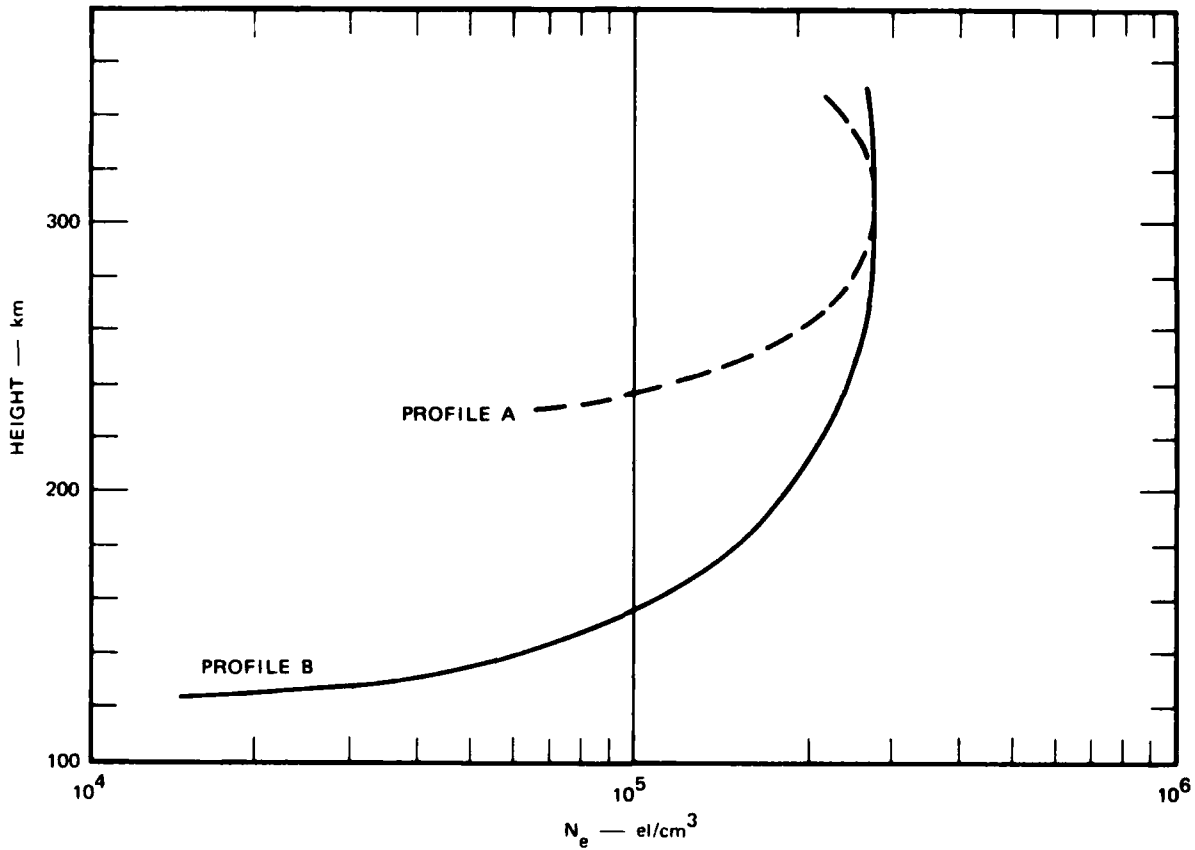


Figure 2. Model electron density profiles.

* C. Rino, personal communication.

incidence critical frequencies of 4.74 MHz at a peak height of 310 km. Profile A has a semithickness of 91 km; Profile B, 191 km. The path also was taken to lie in the geomagnetic meridian plane, as was appropriate for the intended experiment, with a magnetic-dip angle of 80.43 deg. The spatial and temporal correlations and the related quantities calculated for a signal propagated over this path (at a frequency of 10.12 MHz) are shown in Table 3. The 1/e distances given

Table 3. Calculated scatter characteristics for a sample environment

Profile	1/e Distance (m)		1/e Angle (Deg)		Delay Spread (μ s)	1/e Time (ms)	Doppler Spread (Hz)
		⊥		⊥			
A	453.0	32.4	1.2	16.9	290	40.6	7.8
B	624.0	58.9	0.9	9.2	80	73.8	4.3

for the spatial decorrelation are those along the principal axes of the spatial correlation ellipse; for a path in the meridian plane, these axes lie in the plane containing the path (||) and perpendicular to this plane (⊥). The delay spreads given in the last column of the table were calculated from the angular spreads using Eq. 41. The spatial and temporal correlation functions are, according to Eq. 35, Gaussian in these examples by virtue of the value of 1.5 assumed for the power-law index of the spatial irregularity spectrum, and the linearizing assumptions made regarding the path displacement in the derivation of Eq. 33.

As expected, given the magnetic field orientation and the elongation of the irregularities along this field, the angular spreads shown in Table 3 are much larger horizontally than they are in the plane of the path. It is also interesting that Profile B gives smaller spreads in both angle and Doppler than does Profile A. This behavior is consistent with the ray path penetrating to somewhat higher electron

densities for Profile B than for A, as has been confirmed to be the case.

SECTION 9

LIST OF REFERENCES

1. S. M. Flatté, R. Dashen, W. H. Munk, K. M. Watson, and F. Zachariassen, Sound Transmission Through a Fluctuating Ocean (Cambridge University Press, Cambridge, 1979).
2. L. A. Wittwer, "Radio Wave Propagation in Structured Ionization for Satellite Applications," DNA 5504D, Defense Nuclear Agency, Washington, DC (1979).
3. C. L. Rino, "On the Application of Phase Screen Models to the Interpretation of Ionospheric Scintillation Data," Radio Sci., Vol. 17, No. 4, pp. 855-867 (1982).
4. T. A. Croft and H. Hoogasian, "Exact Ray Calculations in a Quasi-parabolic Ionosphere with no Magnetic Field," Radio Sci., Vol. 3, No. 1, pp. 69-74 (1968).
5. R. Esswein and S. M. Flatté, "Calculation of the Phase-structure Function Density from Oceanic Internal Waves," J. Acoust. Soc. Am., Vol. 70, No. 5, pp. 1387-1396 (1981).
6. C. L. Rino, "A Power Law Phase Screen Model for Ionospheric Scintillation. 2. Strong Scatter," Radio Sci., Vol. 14, No. 6, pp. 1147-1155 (1979).
7. L. A. Wittwer, "Radio Wave Propagation in Structured Ionization for Satellite Applications II," DNA-IR-82-02, Defense Nuclear Agency, Washington, DC (1982).

DISTRIBUTION LIST

DEPARTMENT OF DEFENSE

ASSIST SECY OF DEF CMD, CONT, COMM & INTEL
ATTN: DIR OF INTELL SYS

ASSIST TO THE SECY OF DEF
ATTN: EXECUTIVE ASSISTANT

DEFENSE COMMUNICATIONS AGENCY
ATTN: CODE 230
ATTN: J300 FOR YEN-SUN FU

DEFENSE COMMUNICATIONS ENGINEER CENTER
ATTN: CODE R123 TECH LIB
ATTN: CODE R410
ATTN: CODE R410 N JONES

DEFENSE INTELLIGENCE AGENCY
ATTN: RTS-2B

DEFENSE NUCLEAR AGENCY
3 CYS ATTN: RAAE
ATTN: RAAE P LUNN
ATTN: RAAE K SCHWARTZ
ATTN: STNA

4 CYS ATTN: STTI-CA

DEFENSE TECHNICAL INFORMATION CENTER
12 CYS ATTN: DD

FIELD COMMAND DNA DET 2
LAWRENCE LIVERMORE NATIONAL LAB
ATTN: FC-1

FIELD COMMAND DEFENSE NUCLEAR AGENCY
ATTN: FCPR
ATTN: FCTT W SUMMA
ATTN: FCTXE

INTERSERVICE NUCLEAR WEAPONS SCHOOL
ATTN: TTV

JOINT CHIEFS OF STAFF
ATTN: C3S EVAL OFC HDOO

JOINT DATA SYSTEM SUPPORT CTR
ATTN: C-500

JOINT STRAT TGT PLANNING STAFF
ATTN: JLAA
ATTN: JLK ATTN: DNA REP
ATTN: JLKS
ATTN: JPTM

UNDER SECY OF DEF FOR RSCH & ENGRG
ATTN: STRAT & SPACE SYS (OS)

DEPARTMENT OF THE ARMY

BMD ADVANCED TECHNOLOGY CENTER
ATTN: ATC-O W DAVIES
ATTN: ATC-R D RUSS
ATTN: ATC-R W DICKINSON

BMD SYSTEMS COMMAND
ATTN: BMDSC-HW
ATTN: BMDSC-LEH R C WEBB

HARRY DIAMOND LABORATORIES
2 CYS ATTN: SLCHD-NW-P

U S ARMY ATMOSPHERIC SCIENCES LAB
ATTN: SLCAS-AE

U S ARMY COMM-ELEC ENGRG INSTAL AGENCY
ATTN: CC-CE-TP W NAIR

U S ARMY MATERIAL COMMAND
ATTN: DRCLDC J BENDER

U S ARMY NUCLEAR & CHEMICAL AGENCY
ATTN: LIBRARY

U S ARMY STRATEGIC DEFENSE COMMAND
ATTN: DASD-H-L M CAPPS

USA MISSILE COMMAND
ATTN: DRSMI-YSO J GAMBLE

DEPARTMENT OF THE NAVY

NAVAL INTELLIGENCE SUPPORT CTR
ATTN: NISC-50

NAVAL OCEAN SYSTEMS CENTER
ATTN: CODE 532
ATTN: CODE 5322 M PAULSON
ATTN: CODE 5323 J FERGUSON

NAVAL RESEARCH LABORATORY
ATTN: CODE 4187
ATTN: CODE 4700 S OSSAKOW
ATTN: CODE 4720 J DAVIS
ATTN: CODE 6700
ATTN: CODE 7500 B WALD
ATTN: CODE 7950 J GOODMAN

NAVAL SURFACE WEAPONS CENTER
ATTN: CODE F31

OFC OF THE DEPUTY CHIEF OF NAVAL OPS
ATTN: NOP 941D

DEPARTMENT OF THE NAVY (CONTINUED)

SPACE & NAVAL WARFARE SYSTEMS CMD
ATTN: CODE 501A
ATTN: PDE-110-X1 B KRUGER
ATTN: PDE-110-11021 G BRUNHART
ATTN: PME 106-4 S KEARNEY
ATTN: PME 117-20

STRATEGIC SYSTEMS PROGRAMS(PM-1)
ATTN: NSP-2141
ATTN: NSP-2722
ATTN: NSP-43 TECH LIB

THEATER NUCLEAR WARFARE PROGRAM OFC
ATTN: PMS-423 D SMITH

DEPARTMENT OF THE AIR FORCE

AIR FORCE GEOPHYSICS LABORATORY
ATTN: CA/A STAIR
ATTN: LIS J BUCHAU
ATTN: LS
ATTN: LS H GARDINER
ATTN: LS R O'NIEL

AIR FORCE TECHNICAL APPLICATIONS CTR
ATTN: TN

AIR FORCE WEAPONS LABORATORY, AFSC
ATTN: SUL

AIR FORCE WRIGHT AERONAUTICAL LAB/AAAD
ATTN: A JOHNSON
ATTN: W HUNT

AIR UNIVERSITY LIBRARY
ATTN: AUL-LSE

ASSISTANT CHIEF OF STAFF
ATTN: AF/SASC C RIGHTMEYER

BALLISTIC MISSILE OFFICE/DAA
ATTN: ENSN W WILSON
ATTN: SYC D KWAN

DEPUTY CHIEF OF STAFF
ATTN: AFRDS SPACE SYS & C3 DIR

FOREIGN TECHNOLOGY DIVISION, AFSC
ATTN: NIIS LIBRARY

ROME AIR DEVELOPMENT CENTER, AFSC
ATTN: TSLD

STRATEGIC AIR COMMAND
ATTN: SAC/SIJ

STRATEGIC AIR COMMAND
ATTN: NRI/STINFO

STRATEGIC AIR COMMAND
ATTN: XPFS

DEPARTMENT OF ENERGY

DEPARTMENT OF ENERGY GTN
ATTN: DP-233

LAWRENCE LIVERMORE NATIONAL LAB
ATTN: L-31 R HAGER
ATTN: L-53 TECH INFO DEPT. LIBRARY

LOS ALAMOS NATIONAL LABORATORY
ATTN: D SAPPENFIELD
ATTN: D SIMONS
ATTN: G-6 E JONES
ATTN: J WOLCOTT
ATTN: MS 664 J ZINN
ATTN: R JEFFRIES
ATTN: T KUNKLE, ESS-5

SANDIA NATIONAL LABORATORIES
ATTN: D DAHLGREN
ATTN: ORG 1231 R C BACKSTROM
ATTN: ORG 1250 W BROWN
ATTN: ORG 4231 T WRIGHT

OTHER GOVERNMENT

CENTRAL INTELLIGENCE AGENCY
ATTN: OSWR/NED
ATTN: OSWR/SSD FOR K FEUERPFETL

U S DEPARTMENT OF COMMERCE
ATTN: W UTLAUT

DEPARTMENT OF DEFENSE CONTRACTORS

AUSTIN RESEARCH ASSOCIATES
ATTN: J THOMPSON

BERKELEY RSCH ASSOCIATES, INC
ATTN: C PRETTIE
ATTN: J WORKMAN
ATTN: S BRECHT

BOEING CO
ATTN: M/S 6K-92 D CLAUSON

CALIFORNIA RESEARCH & TECHNOLOGY, INC
ATTN: M ROSENBLATT

CALIFORNIA, UNIVERSITY AT SAN DIEGO
ATTN: H BOOKER

ELECTROSPACE SYSTEMS, INC
ATTN: P PHILLIPS

EOS TECHNOLOGIES, INC
ATTN: B GABBARD
ATTN: W LELEVIER

DEPARTMENT OF DEFENSE CONTRACTORS (CONT)

HARRIS CORP

ATTN: E KNICK

HSS, INC

ATTN: D HANSEN

INSTITUTE FOR DEFENSE ANALYSES

ATTN: E BAUER

JAYCOR

ATTN: J SPERLING

KAMAN TEMPO

ATTN: B GAMBILL

ATTN: DASIAC

ATTN: W MCNAMARA

KAMAN TEMPO

ATTN: DASIAC

M I T LINCOLN LAB

ATTN: D TOWLE L-230

MAXIM TECHNOLOGIES, INC

ATTN: J LEHMAN

ATTN: J MARSHALL

ATTN: R MORANSTERN

MCDONNELL DOUGLAS CORP

ATTN: R HALPRIN

ATTN: TECH LIB SVCS

ATTN: W OLSON

METEOR COMMUNICATIONS CORP

ATTN: R LEADER

MISSION RESEARCH CORP

ATTN: C LAUER

ATTN: D KNEPP

ATTN: F FAJEN

ATTN: F GUIGLIANO

ATTN: G MCCARTOR

ATTN: R BIGONI

ATTN: R BOGUSCH

ATTN: R DANA

ATTN: R HENDRICK

ATTN: R KILB

ATTN: S GUTSCHE

ATTN: TECH LIBRARY

MITRE CORP

ATTN: MS J104/M R DRESP

MITRE CORP

ATTN: J WHEELER

ATTN: W FOSTER

ATTN: W HALL

PACIFIC-SIERRA RESEARCH CORP

ATTN: H BRODE, CHAIRMAN SAGE

PHYSICAL DYNAMICS, INC

ATTN: E FREMOUW

PHYSICAL RESEARCH, INC

ATTN: R DELIBERIS

ATTN: T STEPHENS

PHYSICAL RESEARCH, INC

ATTN: J DEVORE

ATTN: J THOMPSON

ATTN: W SCHLUETER

R & D ASSOCIATES

ATTN: F GILMORE

ATTN: M GANTSWEG

ATTN: W KARZAS

ATTN: P HAAS

R & D ASSOCIATES

ATTN: B YOON

R & D ASSOCIATES

ATTN: G GANONG

RAND CORP

ATTN: C CRAIN

ATTN: E BEDROZIAN

ATTN: P DAVIS

RAND CORP

ATTN: B BENNETT

SCIENCE APPLICATIONS INTL CORP

ATTN: D HAMLIN

ATTN: L LINSON

SCIENCE APPLICATIONS INTL CORP

ATTN: M CROSS

SRI INTERNATIONAL

ATTN: C RINO

ATTN: D MCDANIEL

2 CYS ATTN: G PRICE

ATTN: G SMITH

ATTN: J VICKREY

ATTN: R LEADABRAND

ATTN: R TSUNODA

ATTN: W CHESNUT

ATTN: W JAYE

TOYON RESEARCH CORP

ATTN: J GARBARINO

ATTN: J ISE

VISIDYNE, INC

ATTN: J CARPENTER

DISTRIBUTION LIST UPDATE

This mailer is provided to enable DNA to maintain current distribution lists for reports. We would appreciate your providing the requested information.

- Add the individual listed to your distribution list.
- Delete the cited organization/individual.
- Change of address.

NAME: _____

ORGANIZATION: _____

OLD ADDRESS

CURRENT ADDRESS

TELEPHONE NUMBER: () _____

SUBJECT AREA(s) OF INTEREST:

DNA OR OTHER GOVERNMENT CONTRACT NUMBER: _____

CERTIFICATION OF NEED-TO-KNOW BY GOVERNMENT SPONSOR (if other than DNA):

SPONSORING ORGANIZATION: _____

CONTRACTING OFFICER OR REPRESENTATIVE: _____

SIGNATURE: _____

Director
Defense Nuclear Agency
ATTN: STTI
Washington, DC 20305-1000

Director
Defense Nuclear Agency
ATTN: STTI
Washington, DC 20305-1000

END
FILMED

5-86

DTIC